Science Advances
AAAS

advances.sciencemag.org/cgi/content/full/6/6/eaay5247/DC1

Supplementary Materials for

Chromatin accessibility analysis reveals regulatory dynamics of developing human retina and hiPSC-derived retinal organoids

Haohuan Xie, Wen Zhang, Mei Zhang*, Tasneem Akhtar, Young Li, Wenyang Yi, Xiao Sun, Zuqi Zuo, Min Wei, Xin Fang, Ziqin Yao, Kai Dong, Suijuan Zhong, Qiang Liu, Yong Shen, Qian Wu, Xiaoqun Wang, Huan Zhao, Jin Bao, Kun Qu*, Tian Xue*

*Corresponding author. Email: xuetian@ustc.edu.cn (T.X.); qukun@ustc.edu.cn (K.Q.); zhangmei@ustc.edu.cn (M.Z.)

Published 7 February 2020, *Sci. Adv.* **6**, eaay5247 (2020)
DOI: 10.1126/sciadv.aay5247

This PDF file includes:

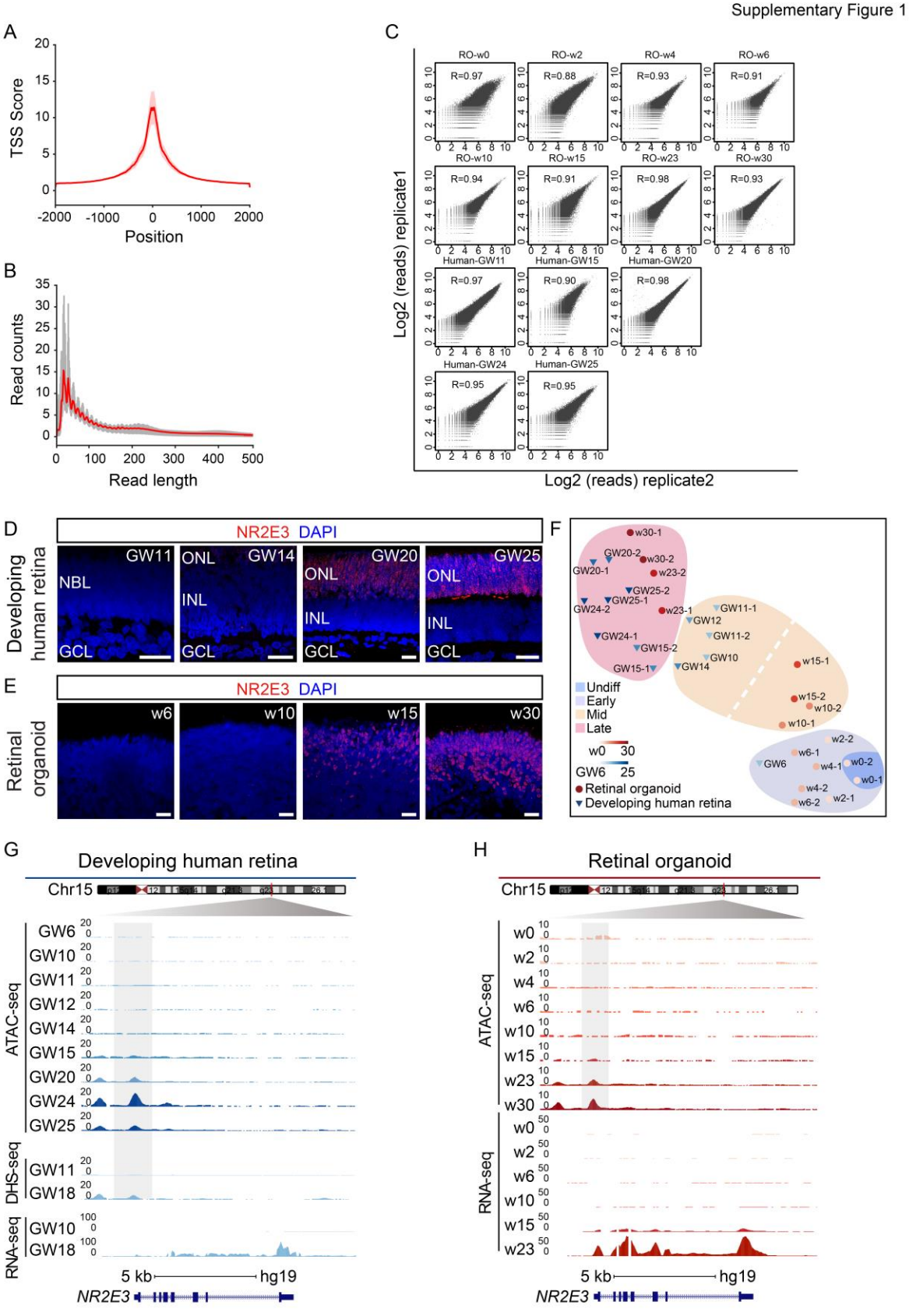
A
TSS Score
Position
B
Read counts
Read length
C
RO-w0
RO-w2
RO-w4
RO-w6
RO-w10
RO-w15
RO-w23
RO-w30
Human-GW11
Human-GW15
Human-GW20
Human-GW24
Human-GW25
Log2 (reads) replicate1
Log2 (reads) replicate2
D
NR2E3 DAPI
Developing human retina
NBL
ONL
INL
GCL
GW11
GW14
GW20
GW25
E
NR2E3 DAPI
Retinal organoid
w6
w10
w15
w30
F
Undiff
Early
Mid
Late
Retinal organoid
Developing human retina
G
Developing human retina
Chr15
ATAC-seq
DHS-seq
RNA-seq
5 kb
hg19
NR2E3
H
Retinal organoid
Chr15
ATAC-seq
RNA-seq
5 kb
hg19
NR2E3

Fig. S1. Qualification of ATAC-seq data. (**A**) Quality control of transcription starting site (TSS) enrichment score of all samples in ATAC-seq data. Red curve indicates the average score for all data. (**B**) Quality control of fragment length distribution of all mapped reads in ATAC-seq data. Red curve indicates the average distribution for all data. (**C**) Scatter plots comparing the ATAC-seq signal between replicate samples in human retinae and ROs. The Pearson correlation coefficients are shown. (**D** and **E**) Immunostaining of NR2E3 (red) in human retinae (D) and ROs (E). Nuclei were stained with DAPI. NBL, neuroblastic layer; ONL, outer nuclear layer; INL, inner nuclear layer; GCL, ganglion cell layer. Scale bar, 20 μm. (**F**) Chromatin accessibility analysis of human retinal and RO development visualized by UMAP with all the ATAC-seq data. Relevant developmental stages are labeled with distinct colors as Fig. 1A. (**G** and **H**) Normalized epigenetic and expression profiles at *NR2E3* loci during human retinal development (G) and RO differentiation (H). All signals were obtained from the UCSC genome browser.

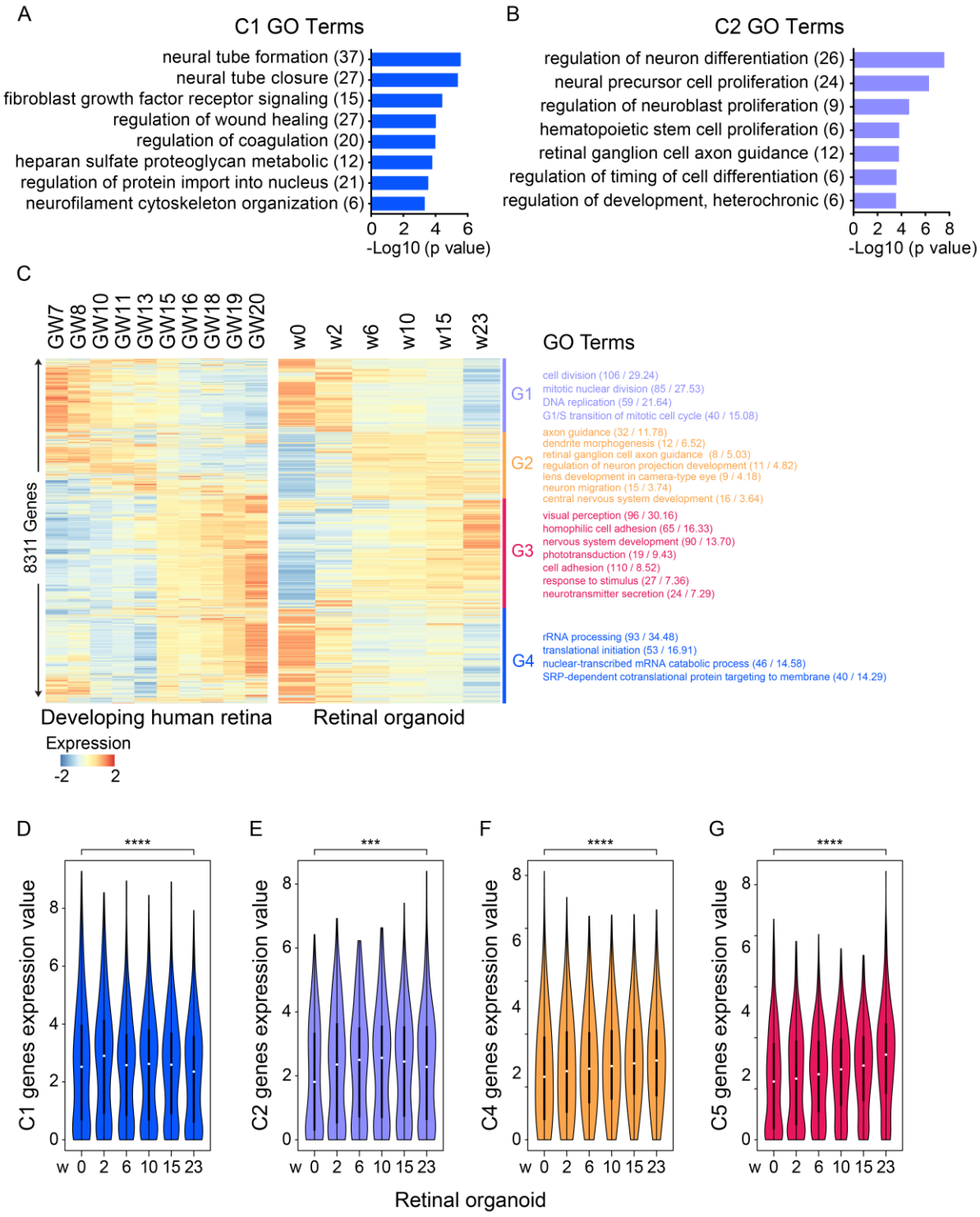
A
C1 GO Terms
neural tube formation (37)
neural tube closure (27)
fibroblast growth factor receptor signaling (15)
regulation of wound healing (27)
regulation of coagulation (20)
heparan sulfate proteoglycan metabolic (12)
regulation of protein import into nucleus (21)
neurofilament cytoskeleton organization (6)
0 2 4 6
-Log10 (p value)
B
C2 GO Terms
regulation of neuron differentiation (26)
neural precursor cell proliferation (24)
regulation of neuroblast proliferation (9)
hematopoietic stem cell proliferation (6)
retinal ganglion cell axon guidance (12)
regulation of timing of cell differentiation (6)
regulation of development, heterochronic (6)
0 2 4 6 8
-Log10 (p value)
C
GW7 GW8 GW10 GW11 GW13 GW15 GW16 GW18 GW19 GW20
w0 w2 w6 w10 w15 w23
8311 Genes
GO Terms
G1
cell division (106 / 29.24)
mitotic nuclear division (85 / 27.53)
DNA replication (59 / 21.64)
G1/S transition of mitotic cell cycle (40 / 15.08)
G2
axon guidance (32 / 11.78)
dendrite morphogenesis (12 / 6.52)
retinal ganglion cell axon guidance (8 / 5.03)
regulation of neuron projection development (11 / 4.82)
lens development in camera-type eye (9 / 4.18)
neuron migration (15 / 3.74)
central nervous system development (16 / 3.64)
G3
visual perception (96 / 30.16)
homophilic cell adhesion (65 / 16.33)
nervous system development (90 / 13.70)
phototransduction (19 / 9.43)
cell adhesion (110 / 8.52)
response to stimulus (27 / 7.36)
neurotransmitter secretion (24 / 7.29)
G4
rRNA processing (93 / 34.48)
translational initiation (53 / 16.91)
nuclear-transcribed mRNA catabolic process (46 / 14.58)
SRP-dependent cotranslational protein targeting to membrane (40 / 14.29)
Developing human retina
Retinal organoid
Expression
-2 2
D
E
F
G
****
***
****
****
C1 genes expression value
C2 genes expression value
C4 genes expression value
C5 genes expression value
0 2 4 6 8
w 0 2 6 10 15 23
Retinal organoid

Fig. S2. Analysis of differential chromatin elements and RNA-seq data in developing human retina and ROs. (**A**) Significant GO terms enriched in C1 cluster peaks using GREAT v3.0.0. The number of genes enriched in GO terms is shown in the parenthesis. (**B**) Significant GO terms enriched in C2 cluster peaks using GREAT v3.0.0. The number of genes enriched in GO terms is shown in the parenthesis. (**C**) Heatmap of 8,311 differentially expressed genes during human retinal development and RO differentiation. Each column is a sample and each row is a gene. Color scale shows relative gene expression levels. GO terms of each cluster are shown on the right with the number of enriched genes and p values (Number of genes/p value). (**D** to **G**) Violin plot representing expression level of genes closest to the top 1,000 peaks in C1 (D), C2 (E), C4 (F) and C5 (G) during RO differentiation showing a variable but positive correlation between chromatin accessibility and gene expression. GREAT was used to annotate peaks to genes. Statistical significance was analyzed with one-way ANOVA, ***$p < 0.001$, ****$p < 0.0001$.

Supplementary Figure 3

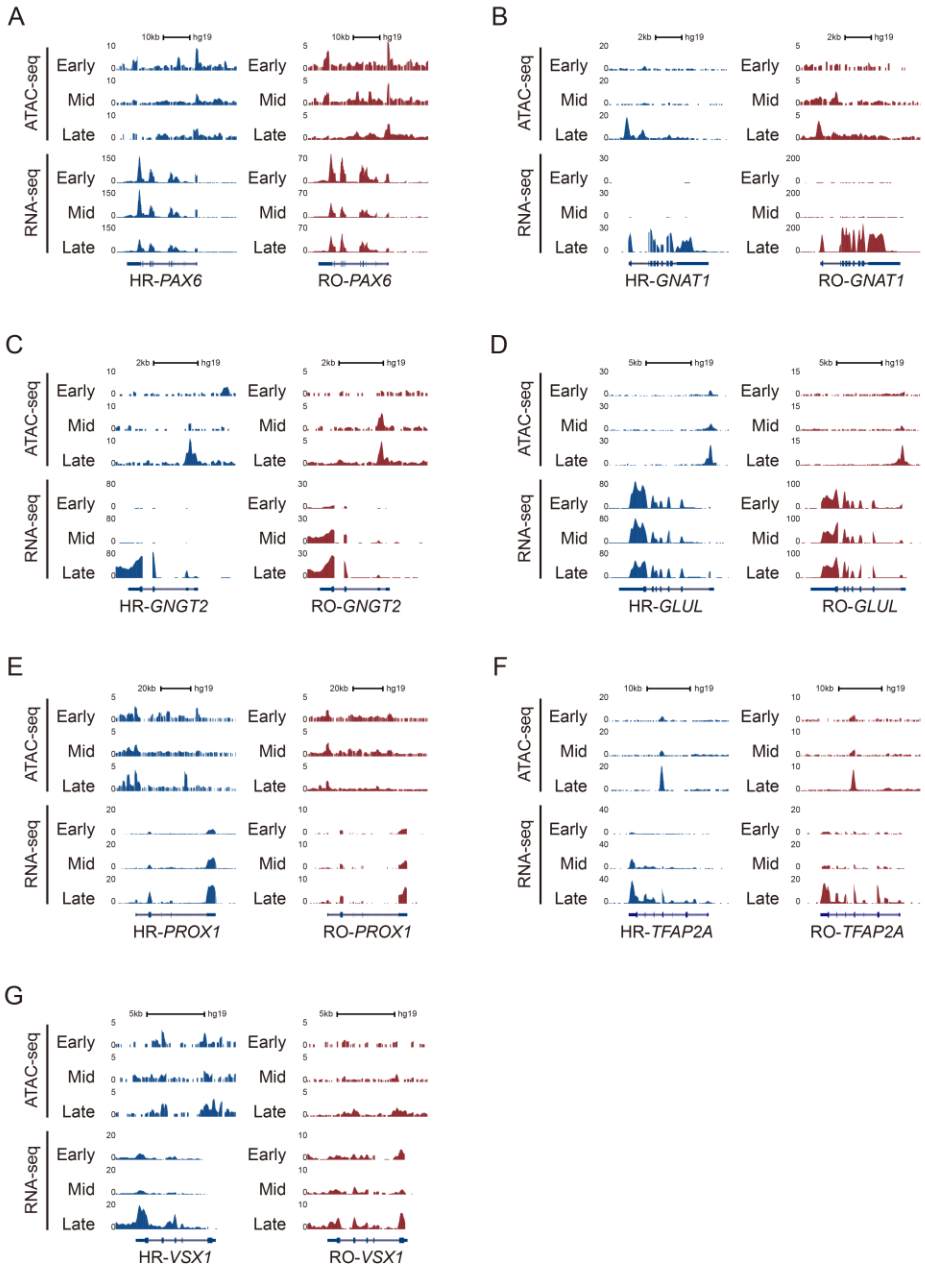

Fig. S3. Epigenetic and expression profiles of retinal cell type markers during retinal development stages. (**A** to **G**) Normalized epigenetic and expression profiles of different retinal cell type markers including *PAX6* for retinal progenitor cells (A), *GNAT1* for rods (B), *GNGT2* for cones (C), *GLUL* for müller cells (D), *PROX1* for horizontal cells (E), *TFAP2A* for amacrine cells (F) and *VSX1* for bipolar cells (G) were shown. All signals were obtained from the UCSC genome browser. Here we chose human GW6, GW10 and GW24 to represent the early, middle and late stages in epigenetic profiles and human GW7, GW10 and GW20 to represent the early, middle and late stages in expression profiles. In RO samples, we chose w6, w15 and w23 to represent the early, middle and late stages in both epigenetic and expression profiles. HR, human retinae; RO, retinal organoids.

Supplementary Figure 4

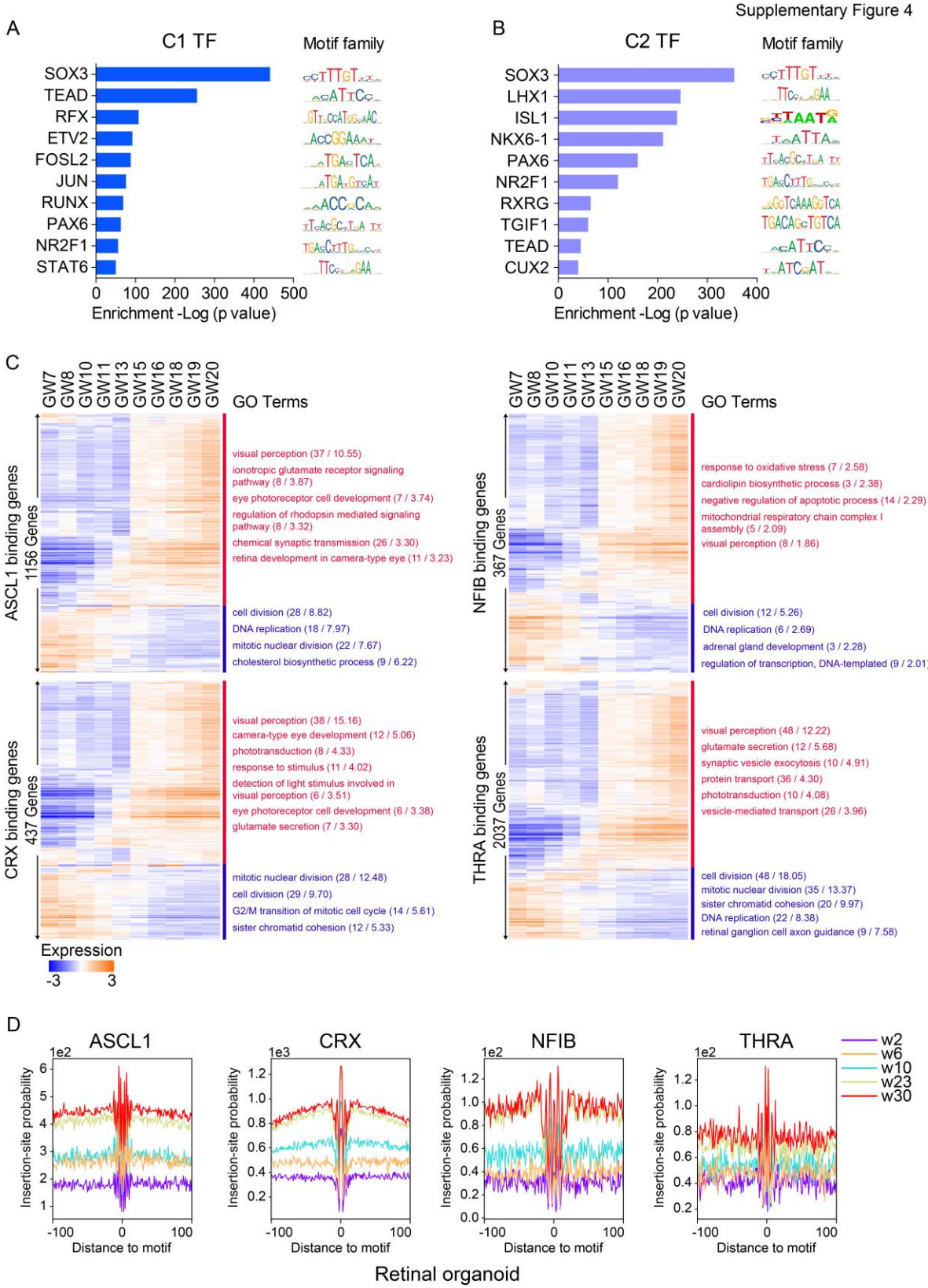

Fig. S4. Identification of putative TFs involved in retinal differentiation. (**A** and **B**) Top ten TF motifs enriched in C1 (A) and C2 (B) cluster peaks, with enrichment p values estimated from HOMER v4.8. (**C**) Heatmaps of expression profiles of genes predicted to be regulated by *ASCL1*, *CRX*, *NFIB*, and *THRA*. Unsupervised hierarchical clustering was performed. Significant GO terms enriched in up- and down-regulated genes are shown on the right with the number of enriched genes and p values (Number of genes/p value). (**D**) Visualization of ATAC-seq footprint for motifs ASCL1, CRX, NFIB, and THRA in ROs at five developmental stages. ATAC-seq signals across all motif binding sites in the C4 and C5 genome regions were aligned on the motif and averaged.

Supplementary Figure 5

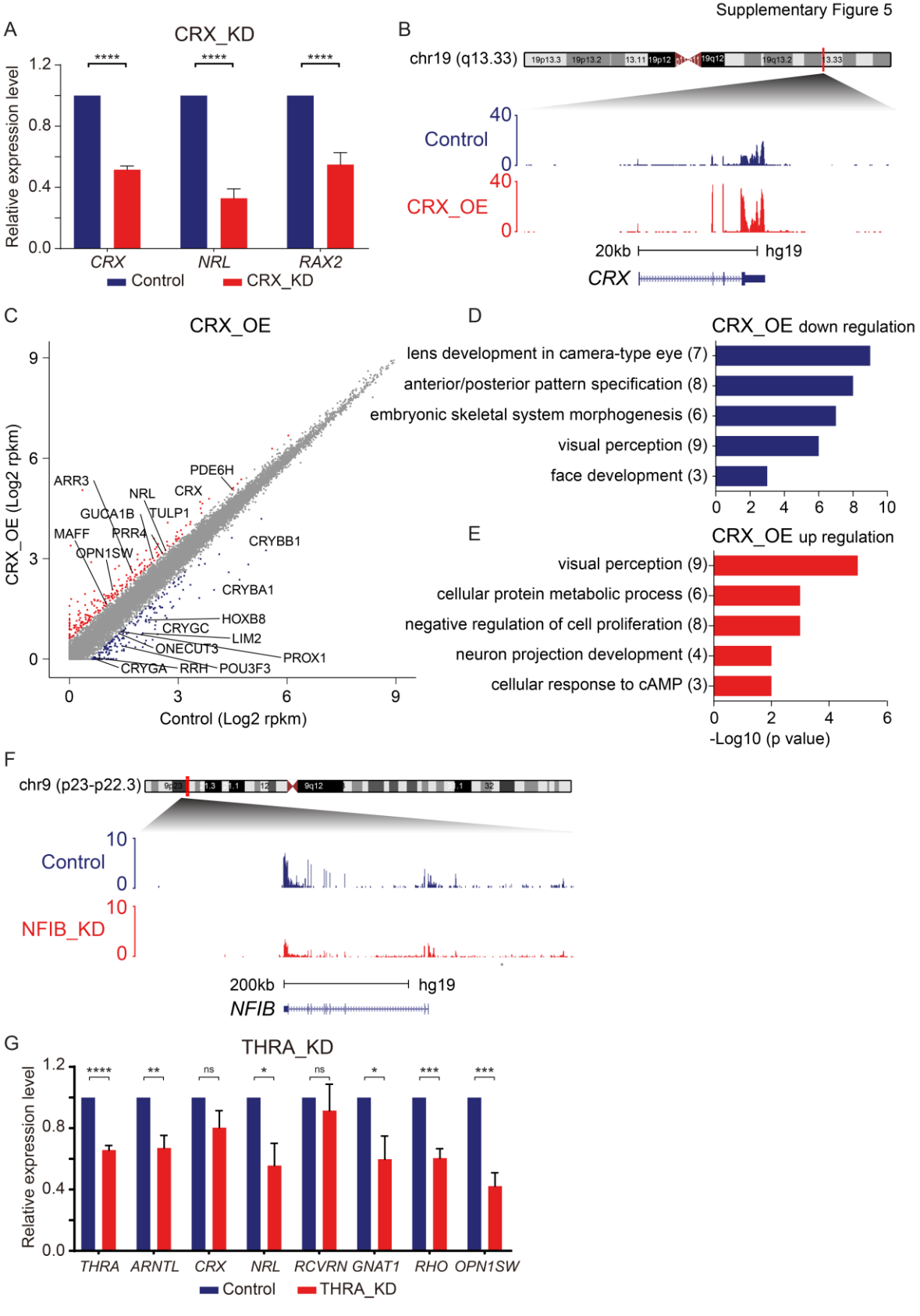

Fig. S5. Functional assay of *THRA* and *NFIB* using RO electroporation. (**A**) qRT-PCR analysis of the target gene expression level after *CRX* knockdown (n = 4). Data are means ± SEM. (**B**) Normalized expression profiles at *CRX* loci between Control and CRX_OE groups. All signals were obtained from the UCSC genome browser. (**C**) Plot representing differentially expressed genes between Control and CRX_OE groups. Significantly up- and down-regulated genes (fold-change > 1.5) are highlighted in red and blue, respectively. (**D** and **E**) Significant GO terms enriched in down- (D) and up- (E) regulated genes, respectively, in CRX_OE experiment. The number of genes enriched in GO terms is shown in the parenthesis. (**F**) Normalized expression profiles at *NFIB* loci between Control and NFIB_KD groups. All signals were obtained from the UCSC genome browser.

(**G**) qRT-PCR analysis of expression levels of genes after knockdown of *THRA* (n = 5). Data are means ± SEM. All statistics by two-tailed Student's t-test; ns, not significant; *p < 0.05, **p < 0.01, ***p < 0.001, ****p < 0.0001.

Supplementary Figure 6

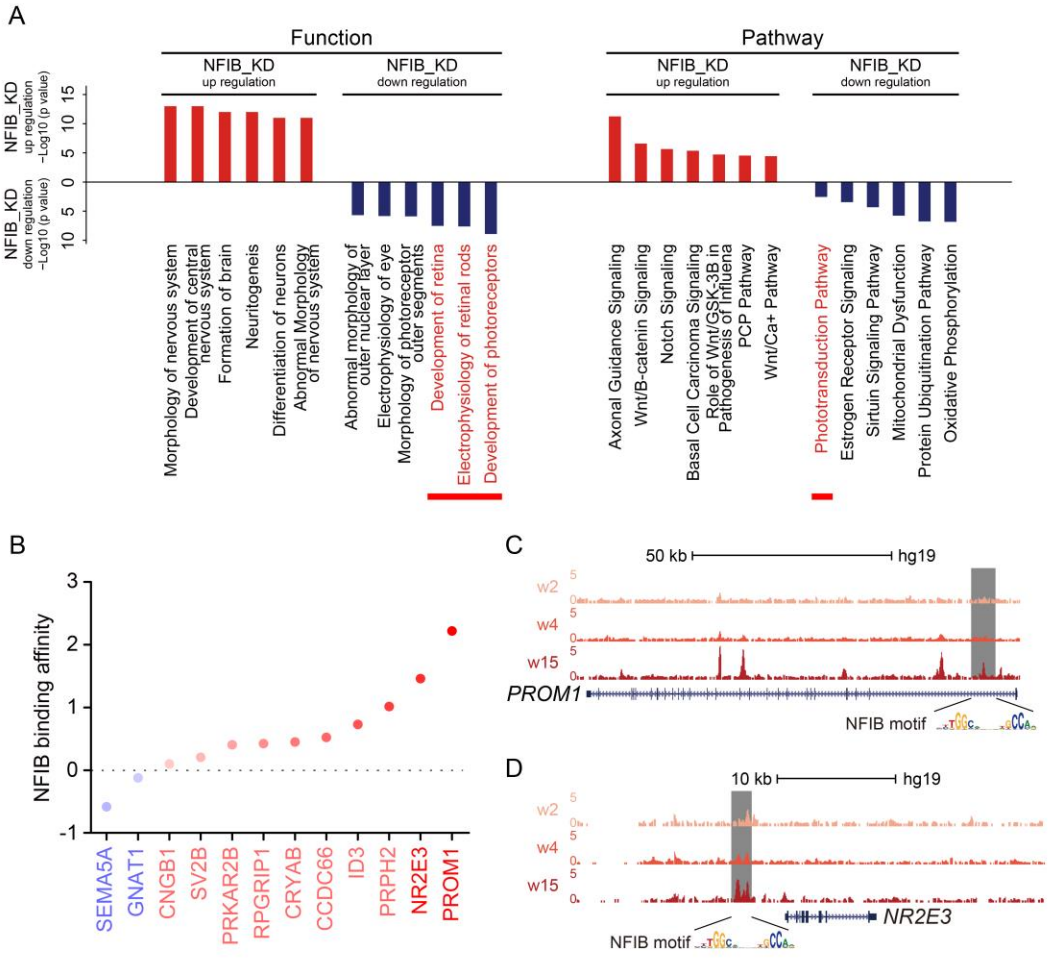

Fig. S6. *NFIB*-regulated signaling pathways in retinal development. (**A**) Significant pathways and functions enriched in down- and up-regulated genes respectively, in NFIB_KD experiment. The result was analyzed with IPA analysis. (**B**) Dot plot showing the potential of genes that may be regulated by *NFIB*. Each dot represents a different gene. (**C** and **D**) Normalized epigenetic profiles at *PROM1* (C) and *NR2E3* (D) loci during RO differentiation. NFIB motif occupying at *PROM1* (C) and *NR2E3* (D) loci, respectively. All signals were obtained from the UCSC genome browser.

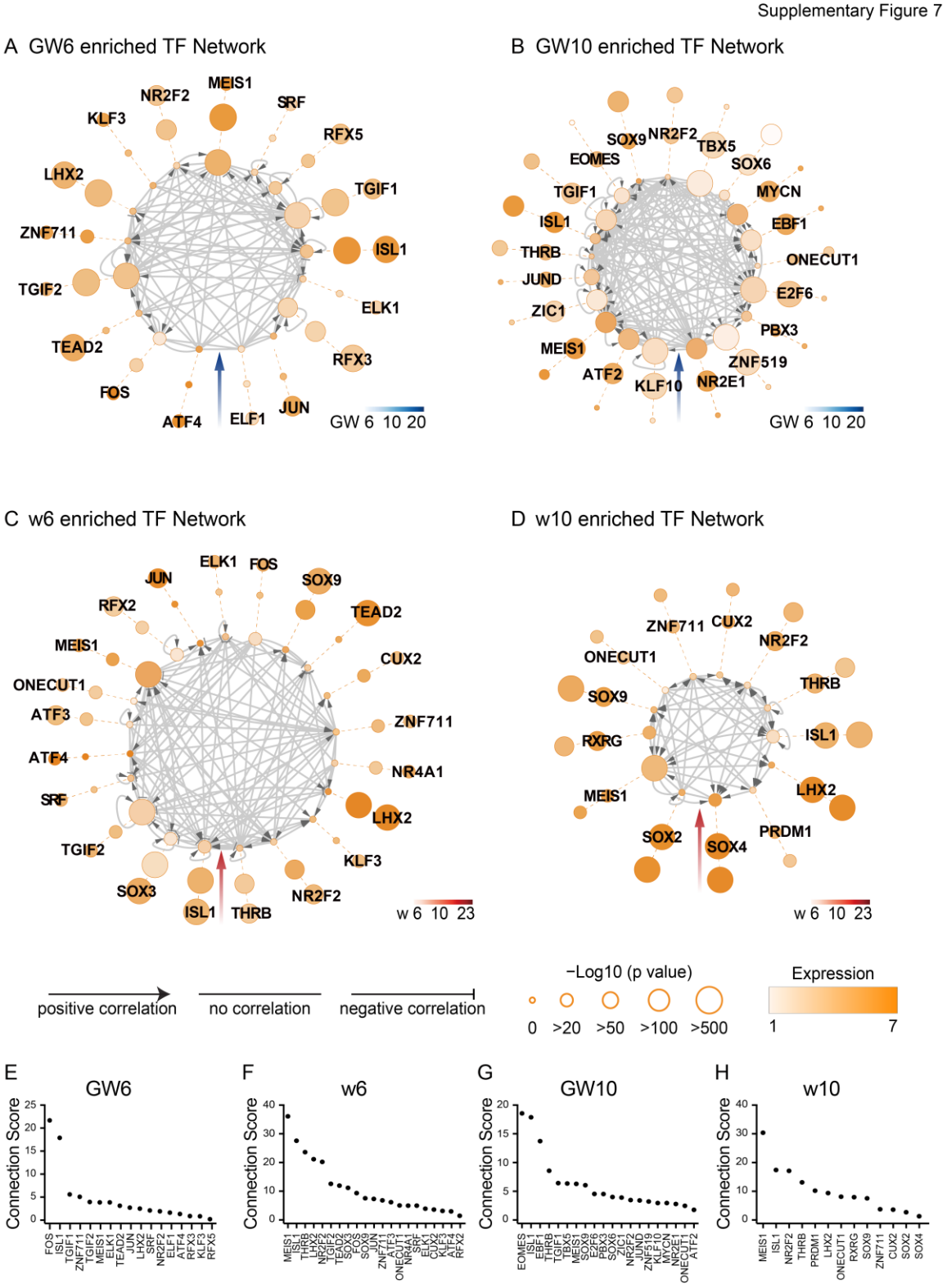
A GW6 enriched TF Network
MEIS1
NR2F2
SRF
KLF3
RFX5
LHX2
TGIF1
ZNF711
ISL1
TGIF2
ELK1
TEAD2
RFX3
FOS
JUN
ATF4
ELF1
GW 6 10 20
B GW10 enriched TF Network
SOX9
NR2F2
TBX5
EOMES
SOX6
TGIF1
MYCN
ISL1
EBF1
THRB
ONECUT1
JUND
E2F6
ZIC1
PBX3
MEIS1
ZNF519
ATF2
KLF10
NR2E1
GW 6 10 20
C w6 enriched TF Network
ELK1
FOS
JUN
SOX9
RFX2
TEAD2
MEIS1
CUX2
ONECUT1
ATF3
ZNF711
ATF4
NR4A1
SRF
LHX2
TGIF2
KLF3
SOX3
NR2F2
ISL1
THRB
w 6 10 23
D w10 enriched TF Network
ZNF711
CUX2
NR2F2
ONECUT1
THRB
SOX9
ISL1
RXRG
LHX2
MEIS1
PRDM1
SOX2
SOX4
w 6 10 23
positive correlation
no correlation
negative correlation
−Log10 (p value)
0 >20 >50 >100 >500
Expression
1 7
E GW6
Connection Score
FOS ISL1 TGIF1 ZNF711 TGIF2 MEIS1 ELK1 TEAD2 JUN LHX2 SRF NR2F2 ELF1 ATF4 RFX3 KLF3 RFX5
F w6
Connection Score
MEIS1 ISL1 THRB LHX2 NR2F2 TGIF2 TGIF1 SOX3 FOS SOX9 JUN ZNF711 ATF3 ONECUT1 NR4A1 SRF ELK1 CUX2 KLF3 ATF4 RFX2
G GW10
Connection Score
EOMES ISL1 EBF1 THRB TBX5 MEIS1 SOX9 E2F6 PBX3 SOX6 ZIC1 NR2F2 JUND ZNF519 KLF10 MYCN NR2E1 ONECUT1 ATF2
H w10
Connection Score
MEIS1 ISL1 NR2F2 THRB PRDM1 LHX2 ONECUT1 RXRG SOX9 ZNF711 CUX2 SOX2 SOX4

Fig. S7. Transcriptional regulatory network during human retinal and RO development. (**A** to **D**) Cis-regulatory networks of TFs in GW6 (A), GW10 (B), w6 (C), and w10 (D). Circle groups from inner to outer represent different time points. Arrow on edge from node *X* to node *Y* indicates that TF-*X* regulates TF-*Y* by binding to the promoter site of the latter. Size of each node indicates TF enrichment and color of each node indicates TF expression levels in that stage. Connection types indicate Pearson correlation between gene expression profiles of connected TFs. (**E** to **H**) Ranking of the connection score in human GW6 (E), GW10 (G) and RO w6 (F), w10 (H) networks. The connection score of each node in the network is calculated as its edge counts multiplied by the standard deviation of its expression.

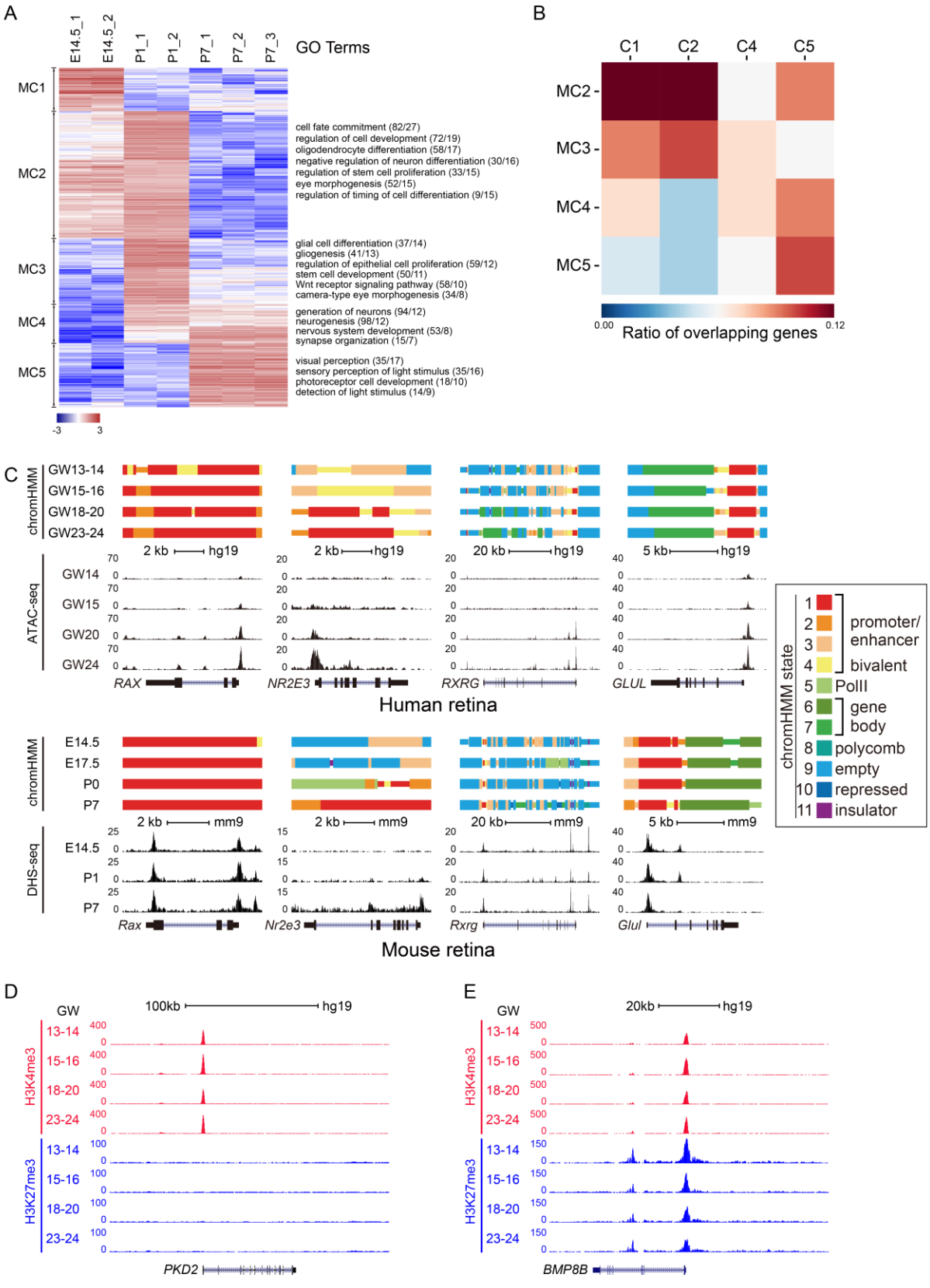
A
E14.5_1
E14.5_2
P1_1
P1_2
P7_1
P7_2
P7_3
GO Terms
MC1
MC2
MC3
MC4
MC5
cell fate commitment (82/27)
regulation of cell development (72/19)
oligodendrocyte differentiation (58/17)
negative regulation of neuron differentiation (30/16)
regulation of stem cell proliferation (33/15)
eye morphogenesis (52/15)
regulation of timing of cell differentiation (9/15)
glial cell differentiation (37/14)
gliogenesis (41/13)
regulation of epithelial cell proliferation (59/12)
stem cell development (50/11)
Wnt receptor signaling pathway (58/10)
camera-type eye morphogenesis (34/8)
generation of neurons (94/12)
neurogenesis (98/12)
nervous system development (53/8)
synapse organization (15/7)
visual perception (35/17)
sensory perception of light stimulus (35/16)
photoreceptor cell development (18/10)
detection of light stimulus (14/9)
-3
3
B
C1
C2
C4
C5
MC2
MC3
MC4
MC5
0.00
0.12
Ratio of overlapping genes
C
chromHMM
GW13-14
GW15-16
GW18-20
GW23-24
2 kb
hg19
20 kb
5 kb
ATAC-seq
GW14
GW15
GW20
GW24
RAX
NR2E3
RXRG
GLUL
Human retina
E14.5
E17.5
P0
P7
mm9
DHS-seq
P1
Rax
Nr2e3
Rxrg
Glul
Mouse retina
chromHMM state
1
2
3
4
5
PolII
6
7
8
polycomb
9
empty
10
repressed
11
insulator
promoter/
enhancer
bivalent
gene
body
D
GW
100kb
hg19
H3K4me3
H3K27me3
13-14
15-16
18-20
23-24
PKD2
E
20kb
BMP8B

Fig. S8. Comparative analyses of human and murine epigenetic data during retinal development. (**A**) Heatmap of differentially regulatory elements during murine retinal development from DHS-seq data. Each column is a sample and each row is a peak region. Color scale shows relative peak intensity levels. GO terms of each cluster are shown on the right with the number of enriched genes and p values (Number of genes/p value). (**B**) The ratio of overlapped gene between human and murine retinal development in distinct clusters. We chose the top 500 peaks in each cluster, and applied GREAT to obtain a list of genes regulated by the ATAC-seq peaks. Ratio is calculated by the number of overlapped genes divided by the gene number of corresponding cluster in mouse. (**C**) ChromHMM states and human ATAC-seq or mouse DHS-seq signals of retinal markers during human retinal development, including *RAX* (retinal progenitors), *NR2E3* (rods), *RXRG* (cones) and *GLUL* (müller cells). Each state is color coded and is used to represent the ChromHMM states (rectangle on the right). (**D** and **E**) Normalized H3K4me3 and H3K27me3 profiles at *PKD2* (D) and *BMP8B* (E) gene loci during human retinal development. All signals were obtained from the UCSC genome browser.

Supplementary Figure 9

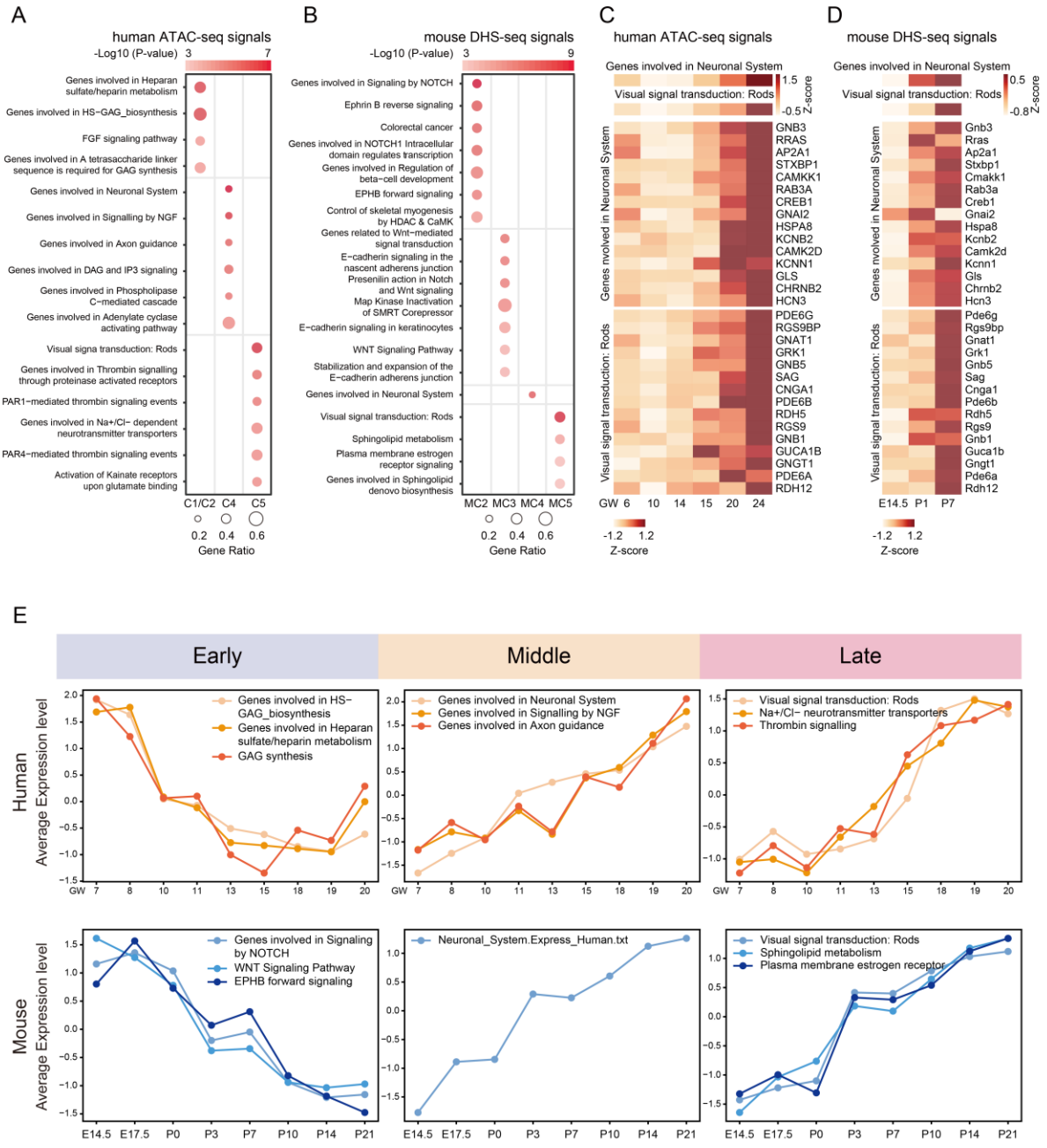

Fig. S9. Signaling pathways in different stages of retinal development in mouse and human. (**A** and **B**) Significant pathways enriched in human (A) and murine (B) retinal development using GREAT v3.0.0. Color of each circle represents the enrichment of the pathway, and the size of the circle represents the ratio of the number of genes in the pathway contained in the cluster to the number of all genes in the corresponding pathway. (**C** and **D**) ATAC-seq signals of pathways and related genes during human (C) and murine (D) retinal development. The ATAC-seq signal of a gene is calculated by average of the signal value of 10 kb upstream and 1 kb downstream for this gene. ATAC-seq signal of a pathway is the average of the signal values of all genes in this pathway. (**E**) The average expression level of genes enriched in each pathway in fig. S9, A and B. during human and murine retinal development.

Table S1. Primers in all experiments.

Name	shRNA Primer sequence
CRX shRNA-F	GATCCCCGGTCTCCGAGCTCCTATTTCATTCAAGAGAT GAAATAGGAGCTCGGAGACCTTTTTG
CRX shRNA-R	AATTCAAAAAGGTCTCCGAGCTCCTATTTCATCTCTTG AATGAAATAGGAGCTCGGAGACCGGG
NFIB shRNA-F	GATCCCCAAGCCACAATGATCCTGCCAAGAATTTCAA GAGAATTCTTGGCAGGATCATTGTGGCTTTTTTTG
NFIB shRNA-R	AATTCAAAAAAAGCCACAATGATCCTGCCAAGAATTC TCTTGAAATTCTTGGCAGGATCATTGTGGCTTGGG
THRA shRNA-F	GATCCCCGGACAAGGCAACTGGTTATCATTCAAGAGA TGATAACCAGTTGCCTTGTCCTTTTTG
THRA shRNA-R	AATTCAAAAAGGACAAGGCAACTGGTTATCATCTCTT GAATGATAACCAGTTGCCTTGTCCGGG
Name	Primers for *CRX* overexpression
CRX cDNA F (BamH I)	GCGCGGATCCATGATGGCGTATATGAACCC
CRX cDNA R (Spe I)	GCGCACTAGTCTACAAGATCTGAAACTTCCAGG
Name	qRT-PCR Primer sequence
beta-ACTIN F	CATGTACGTTGCTATCCAGGC
beta-ACTIN R	CTCCTTAATGTCACGCACGAT
RCVRN F	CCTCTACGACGTGGACGGTAA
RCVRN R	GTGTTTTCATCGTCTGGAAGGA
CRX F	TATTCTGTCAACGCCTTGGCCCTA
CRX R	TGCATTTAGCCCTCCGGTTCTTGA
NRL F	GGCTCCACACCTTACAGCTC
NRL R	GGCCCATCAACAGGGACTG
RAX2 F	GCTCCCACCTTCGCAGATG
RAX2 R	AGCCTGTGCATGTTCCTTGG
NFIB F	AAAAAGCATGAGAAGCGAATGTC
NFIB R	ACTCCTGGCGAATATCTTTGC
EZH2 F	AATCAGAGTACATGCGACTGAGA
EZH2 R	GCTGTATCCTTCGCTGTTTCC
THRA F	AGGTCACCAGATGGAAAGCG
THRA R	AGTGATAACCAGTTGCCTTGTC
ARNTL F	CATTAAGAGGTGCCACCAATCC
ARNTL R	TCATTCTGGCTGTAGTTGAGGA
GNAT1 F	CACGATGCCCAAGGAGATGT
GNAT1 R	GGTGGTTGCAGATGCTGTTG
RHO F	ACAGGATGCAATTTGGAGGGC
RHO R	GCTCATGGGCTTACACACCA
OPN1SW F	CCTGGCTACCTGGACCATTG
OPN1SW R	TAGGACTCGCTGCGGTATTTG